interesting to determine whether the *Brassica oleracea* var. *botrytis AP1* gene is also nonfunctional. Additional experiments, such as complementation of the *cauliflower* phenotype in *botrytis*, will further define the role of *BobCAL* in this crop plant.

REFERENCES AND NOTES

1. E. A. Schultz and G. W. Haughn, *Plant Cell* **3**, 771 (1991); D. Weigel, J. Alvarez, D. R. Smyth, M. F. Yanofsky, E. M. Meyerowitz, *Cell* **69**, 843 (1992); S. Shannon and D. R. Meeks-Wagner, *Plant Cell* **5**, 639 (1993).
2. J. L. Bowman, J. Alvarez, D. Weigel, E. M. Meyerowitz, D. R. Smyth, *Development* **119**, 721 (1993).
3. V. F. Irish and I. M. Sussex, *Plant Cell* **2**, 741 (1990).
4. Z. Schwarz-Sommer, P. Huijser, W. Nacken, H. Saedler, H. Sommer, *Science* **250**, 931 (1990).
5. M. F. Yanofsky *et al.*, *Nature* **346**, 35 (1990); T. Jack, L. L. Brockman, E. M. Meyerowitz, *Cell* **68**, 683 (1992).
6. H. Ma, M. F. Yanofsky, E. M. Meyerowitz, *Genes Dev.* **5**, 484 (1991).
7. M. A. Mandel, C. Gustafson-Brown, B. Savidge, M. F. Yanofsky, *Nature* **360**, 273 (1992).
8. A 4.8-kb Eco RI genomic fragment that hybridized with an *AP1* probe was cloned and sequenced. The corresponding complementary DNA (pBS85) was cloned by reverse transcription–polymerase chain reaction (RT-PCR) with the oligos AGL10-1 (5′-GATCGTCGTTATCTCTCTTG-3′) and AGL10-12 (5′-GTAGTCTATTCAAGCGGCG-3′).
9. Restriction fragment length polymorphism mapping filters were scored and the results analyzed with the Macintosh version of the Mapmaker program as described (*18*), placing *CAL* on the upper arm of chromosome 1 near marker λ235.
10. A 5850–base pair (bp) Bam HI fragment containing the entire coding region of the *Arabidopsis CAL* gene as well as 1860 bp upstream of the putative translational start site was inserted into the pBIN19 plant transformation vector (Clontech) and used for transformation of root tissue from *cal-1 ap1-1* plants as described (*19*). Seeds were harvested from primary transformants, and all phenotypic analyses were performed in subsequent generations.
11. B. Savidge and M. F. Yanofsky, unpublished material.
12. Seeds homozygous for the *ap1-1* allele in L*er* were mutagenized with 0.1% or 0.05% ethylmethane sulfonate (EMS) for 16 hours. Putative new *cal* alleles were crossed to *cal-1 ap1-1 chlorina* plants to verify allelism. Two sets of oligonucleotides were used to amplify and clone new alleles: oligos AGL10-1 and AGL10-2 (5′-GATGGAGACCATTAAACAT-3′) for the 5′ portion and oligos AGL10-3 (5′-GGAGAAGGTACTAGAACG-3′) and AGL10-4 (5′-GCCCTCTTCCATAGATCC-3′) for the 3′ portion of the gene. All coding regions and intron-exon boundaries of the mutant alleles were sequenced.
13. ^{35}S-labeled antisense *CAL* and *BoCAL* mRNAs were synthesized from Sca I–digested cDNA templates and hybridized to 8-μm sections of *Arabidopsis* L*er* or *B. oleracea* inflorescences. The probes do not contain any MADS-box sequences in order to avoid cross-hybridization with other MADS-box genes. Hybridization conditions were the same as previously described (*20*).
14. C. Gustafson-Brown, B. Savidge, M. F. Yanofsky, *Cell* **76**, 131 (1994).
15. S. H. Yarnell, *Bot. Rev.* **22**, 81 (1956); S. Sadik, *Am. J. Bot.* **49**, 290 (1962).
16. The single-copy *BobCAL* gene (Snowball Y Improved, NK Lawn & Garden, Minneapolis, MN) was isolated from a size-selected genomic library in λBlueStar (Novagen) on a 16-kbp Bam HI fragment with the *Arabidopsis CAL* gene as a probe. The *BoCAL* gene was isolated from a rapid cycling line (*21*) by PCR on both RNA and genomic DNA. The cDNA was isolated by RT-PCR with the oligos Bob1 (5′-TCTACGAGAAATGGGAAGG-3′) and Bob2 (5′-GTCGATATATGGCGAGTCC-3′). The 5′ portion of the gene was obtained with oligos Bob1 and Bob4B (5′-CCATTGACCAGTTCGTTTG-3′). The 3′ portion was obtained with oligos Bob3 (5′-GCTCCAGACTCTCACGTC-3′) and Bob2.
17. M. A. Mandel and M. F. Yanofsky, unpublished material.
18. R. S. Rieter *et al.*, *Proc. Natl. Acad. Sci. U.S.A.* **89**, 1477 (1992).
19. D. Valvekens, M. Van Montagu, M. Van Lijsebettens, *ibid.* **85**, 5536 (1988).
20. G. N. Drews, J. L. Bowman, E. M. Meyerowitz, *Cell* **65**, 991 (1991).
21. P. H. Williams and C. B. Hill, *Science* **232**, 1385 (1986).
22. D. R. Smyth, J. L. Bowman, E. M. Meyerowitz, *Plant Cell* **2**, 755 (1990).

23. We thank D. Weigel, M. A. Mandel, and J. Dutra for their assistance and T. Araki, J. Bowman, M. A. Mandel, and D. Weigel for critical comments on the manuscript. Supported by grants from the National Science Foundation (DCB-9018749), the Arnold and Mabel Beckman Foundation, and by a David and Lucile Packard Fellowship in Science and Engineering to M.F.Y. B.S. was supported by National Institutes of Health training grant GM07313.

5 August 1994; accepted 26 October 1994

Mutations of Keratinocyte Transglutaminase in Lamellar Ichthyosis

Marcel Huber, Irmingard Rettler, Katja Bernasconi, Edgar Frenk, Sjan P. M. Lavrijsen, Maria Ponec, Anita Bon, Stefan Lautenschlager, Daniel F. Schorderet, Daniel Hohl*

Lamellar ichthyosis is a severe congenital skin disorder characterized by generalized large scales and variable redness. Affected individuals in three families exhibited drastically reduced keratinocyte transglutaminase (TGK) activity. In two of these families, expression of *TGK* transcripts was diminished or abnormal and no TGK protein was detected. Homozygous or compound heterozygous mutations of the *TGK* gene were identified in all families. These data suggest that defects in TGK cause lamellar ichthyosis and that intact cross-linkage of cornified cell envelopes is required for epidermal tissue homeostasis.

Autosomal recessive lamellar ichthyosis (LI) is a congenital disorder of keratinization [MIM (Mendelian Inheritance in Man) 242100, estimated incidence 1:250,000]. Neonates are often born encased in a tough and inelastic film-like membrane that fissures easily, resulting in a high risk of sepsis and dehydration. Within 2 weeks the membrane sheds, revealing a lifelong disfiguring disease characterized by generalized large scales and variable redness of the skin (*1*). The renewal rate of proliferative basal keratinocytes is strongly enhanced in affected individuals, and this is manifested as thickened epidermis and increased nail and hair growth (*2*). The genetic origin of LI is unknown, and the absence of biological or molecular markers has contributed to disagreements on classification of the disease (*1*).

Transglutaminases (TGs) are a superfamily of enzymes that catalyze transamidation of glutamine residues, a reaction associated with a wide variety of physiological processes such as blood clotting, cytoplasmic coagulation in apoptosis, keratinization, hair follicle formation, fertilization, and dimerization of interleukin-2 in nerves (*3*). The keratinocyte form of TG (TGK) mediates N^{ε}-(γ-glutamyl)lysine cross-linkage (*4*) during formation of the cornified cell envelope (CE), a distinct and highly insoluble structure of 15-nm thickness that replaces the plasma membrane (PM) in terminally differentiating keratinocytes (*5*). This process involves the sequential cross-linking of CE precursor proteins such as involucrin; small, proline-rich proteins; and loricrin on the inner side of the PM (*5*). Simultaneously, the PM is replaced by Ω-hydroxyacyl-sphingosine lipids covalently bound to the outer surface of the protein CE (*5*). TGK is mostly expressed on the PM in upper spinous and granular cell layers of stratified squamous epithelia (*4*). About 5 to 10% of TGK activity is found in the cytoplasmic fraction and may account for the final steps of CE cross-linkage (*4*). TGK activity requires a catalytic thiol center in the enzyme and is sensitive to Ca^{2+} (*3*). The human *TGK* gene has at least two sequence variants, contains 15 exons, and is located on chromosome 14q11 (*TGM1* locus) (*6*).

In previous work, we observed that affected individuals in two families with LI

M. Huber, I. Rettler, K. Bernasconi, E. Frenk, D. Hohl, Laboratory of Cutaneous Biology, Department of Dermatology, Centre Hospitalier Universitaire Vandois (CHUV), Hôpital de Beaumont, CH-1011 Lausanne, Switzerland.
S. P. M. Lavrijsen and M. Ponec, Department of Dermatology, University Hospital of Leiden, Rijnsburgerweg 10, 2333 AA Leiden, Netherlands.
A. Bon and S. Lautenschlager, Municipal Dermatology Clinic, CH-8000 Zürich, Switzerland.
D. F. Schorderet, Unit of Molecular Genetics and Department of Medical Genetics, CHUV, CH-1011 Lausanne, Switzerland.

*To whom correspondence should be addressed.

(LI-1, -2) did not express TGK and showed increased cytoplasmic expression of involucrin and loricrin (*7*). Thus, we speculated that alterations of TGK in LI might alter the cross-linkage of loricrin and involucrin, resulting in an abnormal CE. To investigate TGK function in LI, we performed linkage analysis in three families (LI-1, -2, -3) using a microsatellite located within the *TGM1* locus on chromosome 14q11 (*8*). Although the families were too small to prove linkage, we confirmed that *TGK* was a strong candidate gene. All families showed a perfect match of alleles with two obligate carrier parents and recessive inheritance of LI without recombination (Fig. 1).

Keratinocyte cultures were established from the five affected probands in these families. The cells were grown in the presence of high Ca^{2+} concentrations, a condition normally associated with high levels of involucrin and TGK expression. Membrane-bound TGK activity (*9*) was reduced to 0.8 to 2.8% of normal in all affected probands (Table 1). LI-3.7 and LI-3.8 exhibited an increased ratio of cytosolic to membrane-bound activity. Immunohistochemical studies revealed increased cytoplasmic staining of TGK in LI-3 (*10*). Immunoblot analysis of cytoplasmic and membrane extracts from differentiating keratinocytes (*11*) revealed no detectable TGK in probands of LI-1 and LI-2, and TGK of normal size (92 kD) in LI-3 that was more abundant in the cytoplasmic fraction (Fig. 2A).

We also investigated the three families by Northern (RNA) blot analysis (Fig. 2B) (*12*). In patient LI-1.5, no *TGK* transcripts were detected in total RNA from cultured keratinocytes or from a biopsy. Both patients from family LI-2 showed 2.9- and 2-kb *TGK* transcripts when the blots were hybridized with probes from the 3′ noncoding end or the middle of the *TGK* complementary DNA (cDNA) (3′NC and DH36) and transcripts of 2.9 and 1.0 kb when the probe was from the 5′ end of the cDNA (DH42). *TGK* mRNA of normal size (2.7 kb) was detected in the affected individuals of LI-3.

In proband LI-1.5, single-strand conformation polymorphism (SSCP) and sequence analysis of polymerase chain reaction (PCR) products (*13*) showed a homozygous deletion of a T at position +4640 (*6*) in exon 8 of the *TGK* gene (Fig. 3A). This change leads to a shift in the reading frame and a truncated protein of 442 amino acids that still contains the active site but not the putative Ca^{2+}-binding region (*3*). This mutation also strongly reduced the level of normal transcripts [detectable only by reverse transcriptase–PCR (RT-PCR)] (*10*, *14*) as reported for nonsense and frameshift mutations in other genes (*15*).

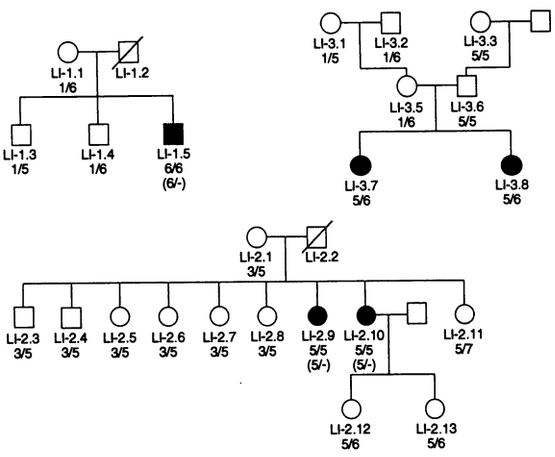

Fig. 1. Pedigrees of the LI families. Clinically, LI-1.5 and LI-2.9 exhibited the nonerythrodermic variant of LI, and LI-2.10, LI-3.7, and LI-3.8 the erythrodermic. The results of the microsatellite analysis (*8*) are shown as numbers below each individual. Marker alleles in parentheses indicate the possibility that the patients of LI-1 and LI-2 inherited a large deletion of the paternal allele at the *TGM1* locus.

Table 1. TG activity in keratinocytes from LI families. Activity is presented as disintegrations per minute per milligram of protein (*9*). Results are given as the mean ± SD from two different cell passages measured in duplicate. Only one cell passage was measured for LI-1.5 because this cell line was nonviable after first passage.

Sample	Activity ($\times 10^{-4}$)		
	Cytosolic	Membrane	Cytosolic:membrane
LI-1.5	0.33	4.0	0.08
LI-2.9	0.72 ± 0.1	6.3 ± 1.0	0.11
LI-2.10	1.1 ± 0.3	6.5 ± 3.0	0.17
LI-3.7	1.95 ± 0.4	5.0 ± 1.0	0.39
LI-3.8	1.90 ± 1.4	1.8 ± 1.0	1.00
N1*	29.3 ± 2.4	247 ± 57	0.11
N2*	19.2 ± 3.2	221 ± 97	0.09

*N1 and N2, healthy controls.

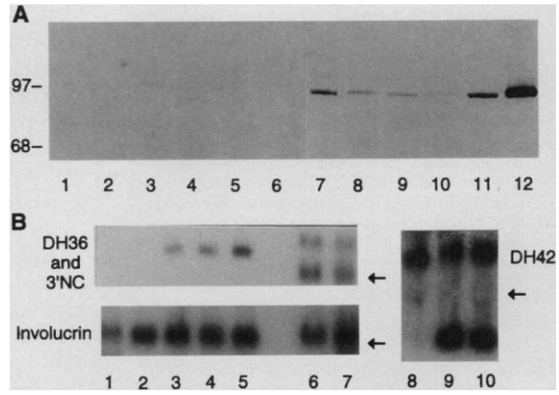

Fig. 2. (**A**) Immunoblot of cytosolic (lanes 1, 3, 5, 7, 9, and 11) and membrane (lanes 2, 4, 6, 8, 10, and 12) extracts from patients LI-1.5 (lanes 1 and 2), LI-2.10 (lanes 3 and 4), LI-2.9 (lanes 5 and 6), LI-3.7 (lanes 7 and 8), LI-3.8 (lanes 9 and 10), and unaffected individual (lanes 11 and 12). Protein (40 μg) from each extract was run on a 10% SDS-polyacrylamide gel as in (*4*). Antibody B.C1 (*4*) and the ECL kit (Amersham) were used for immunodetection. Note abundant protein in cytosolic fractions of LI-3.7 and LI-3.8. Molecular sizes are indicated at left (in kilodaltons). (**B**) Northern blot analysis of total RNA (13 μg) from LI patients isolated from skin biopsy (lane 1) or cell cultures (lanes 2 to 10) with different cDNA probes (*12*). Lanes 1 and 2, LI-1.5; lane 3, LI-3.8; lane 4, LI-3.7; lanes 5 and 8, unaffected individual; lanes 6 and 9, LI-2.10; lanes 7 and 10, LI-2.9. Arrows show position of 18S ribosomal RNA.

Affected individuals of LI-2 showed a homozygous A to G change at position +3366 (*6*, *13*) that converted the canonical splice acceptor sequence 5′-CCTCCTTCCAG-3′ of intron 5 in the wild-type allele into the sequence 5′-CCTCCTTCCGG-3′ (Fig. 3B). The cDNA products (*14*) obtained from LI-2.9 and LI-2.10 RNA showed the same A to G change found in genomic DNA and contained the complete intron 5 sequence inserted into the normal transcript. This inclusion of intron 5 leads to a shift in the reading frame and creates a premature stop codon upstream of the sequences coding for the active site of the TGK enzyme. Retention of intron 5 explains the slightly larger band observed in Northern blot analysis of LI-2.9 and LI-2.10. A similar finding was reported for an A to G mutation in the 3′ splice site

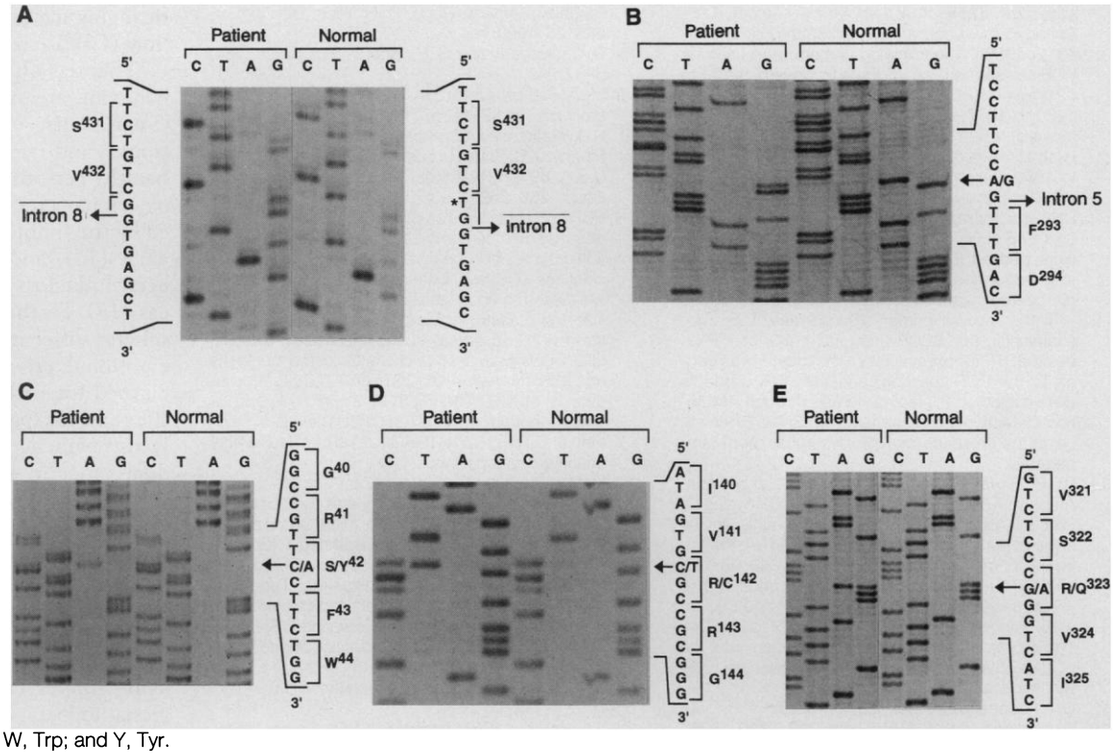

Fig. 3. Sequence analysis of the *TGK* gene in LI families. Normal, sequence obtained from an affected individual; Patient, sequence from an unaffected person. The nucleotide and amino acid sequences have been numbered as in (*6*). (**A**) Homozygous deletion of a T (indicated by an asterisk) at position +4640 in affected individual of LI-1. (**B**) Homozygous A to G substitution at position +3366 in LI-2.9 and -2.10. (**C**) Heterozygous C to A change at +950 in affected individuals of LI-3. (**D**) Heterozygous C to T substitution at +1399 in affected individuals of LI-3. (**E**) Heterozygous G to A substitution at +3459 in affected individuals of LI-3. Single-letter abbreviations for the amino acid residues are as follows: C, Cys; D, Asp; F, Phe; G, Gly; I, Ile; Q, Gln; R, Arg; S, Ser; V, Val; W, Trp; and Y, Tyr.

of intron 3 in the *ApoE* gene in familial apoE deficiency (*16*). The 2- and 1-kb mRNAs seen on Northern blots might arise when there is correct cleavage at the 5′ splice site of intron 5 without excision of the intron. Neither of their translation products is likely to be functional.

Both affected probands of the LI-3 family exhibited three mutations of the *TGK* gene (*13*). The first mutation involves a C to A transversion at position +950 (6) (exon 2, inherited from father) changing Ser^{42} to Tyr (Fig. 3C). This residue may be a site for phosphorylation (*17*) and is five amino acids upstream of the Cys cluster thought to be the membrane anchor region of TGK (*18*). Mutational analysis has shown that regions adjacent to the Cys cluster are also important for membrane attachment of TGK (*19*). This might explain the increased ratio of cytosolic to membrane TGK activity and protein in these patients (Table 1 and Fig. 2A). The second (exon 3, inherited from father) and third mutations (exon 6, inherited from mother) were a C to T change at position +1399 (6) (Fig. 3D) and a G to A change at position +3459 (Fig. 3E), leading to replacement of Arg^{142} with Cys and Arg^{323} with Gln, respectively. Both Arg residues are located within regions highly conserved in all TG sequences (*20*).

Analysis of the mutations in all family members of LI-1, -2, and -3 (*21*) showed a perfect match with the observed inheritance of microsatellite marker alleles (Fig. 1). Screening of genomic DNA samples from 50 randomly selected healthy individuals revealed no carriers for the mutations found in families LI-1 and LI-3. One heterozygous carrier of the A to G mutation at +3366 was detected in 300 randomly selected healthy individuals. This frequency predicts a risk for homozygosity of 1 in 360,000, but might be lower. No DNA was available from the fathers LI-1.2 and LI-2.2. Thus, we cannot formally exclude in these kindreds either uniparental isodisomy of the maternal allele or a very large deletion of the paternal allele at the *TGM1* locus.

The correlation of TGK activity loss with the mutations identified in these LI patients suggests that faulty TGK causes a thickened epidermis and scales. Thus, intact cross-linkage of precursor proteins forming mature CE contributes to the maintenance of a functional epidermis. The pathological keratinization in LI might also arise as a result of abnormal covalent binding of Ω-hydroxyacyl-sphingosine lipids on the outer surface of cornified cell envelopes. Several mutations have been reported to cause reduced transglutaminase activity in congenital deficiency of coagulation factor XIIIa (*22*), suggesting that other mutations will be discovered in conserved regions of TGK.

Note added in proof: Since the submission of this work, Russell *et al.* reported complete linkage of lamellar ichthyosis in 13 families with several markers mapping to chromosome 14q11 [*Am. J. Hum. Genet.* **55**, 1146 (1994)].

REFERENCES AND NOTES

1. S. B. Phillips and H. P. Baden, in *Dermatology in General Medicine*, T. Fitzpatrick, A. Eisen, K. Wolff, I. Freedberg, K. Austen, Eds. (McGraw-Hill, New York, 1993), chap. 42; H. Traupe, *The Ichthyoses* (Springer, Berlin, 1989), pp. 111–134.
2. P. Frost and E. Van Scott, *Arch. Dermatol.* **94**, 113 (1966).
3. C. S. Greenberg, P. J. Birckbichler, R. H. Rice, *FASEB J.* **5**, 3071 (1991); S. Eitan and M. Schwartz, *Science* **261**, 106 (1993); K. Ho, V. E. Quarmby, F. S. French, E. M. Wilson, *J. Biol. Chem.* **267**, 12660 (1992).
4. S. M. Thacher and R. H. Rice, *Cell* **40**, 685 (1985); S. M. Thacher, *J. Invest. Dermatol.* **92**, 578 (1989).
5. U. Reichert, S. Michel, R. Schmidt, in *Molecular Biology of the Skin*, M. Darmon and M. Blumenberg, Eds. (Academic Press, New York, 1993), chap 4; D. Hohl and D. Roop, *ibid.*, chap 5.
6. M. A. Phillips, B. E. Stewart, R. H. Rice, *J. Biol. Chem.* **267**, 2282 (1992); I. Kim *et al.*, *ibid.*. p. 7710.
7. D. Hohl, M. Huber, E. Frenk, *Arch. Dermatol.* **129**, 618 (1993); A. P. M. Lavrijsen and T. Maruyama, *ibid.*, in press.
8. PCR-based microsatellite assays for a dinucleotide repeat polymorphism in the *TGM1* locus (*6*) were performed with forward [nucleotides (nt) 12980 to 13009] and reverse primers (nt 13139 to 13168). Thirty cycles were performed at 94°C, 1 min; 65°C, 1 min; 72°C, 1 min; and a final extension at 72°C for 10 min. PCR products were separated on an ALF automatic sequencing system and were analyzed with Fragment Manager version 1.1 (Pharmacia LKB Biotechnology).
9. U. Lichti, T. Ben, S. H. Yuspa, *J. Biol. Chem.* **260**, 1422 (1985).
10. M. Huber *et al.*, unpublished data.
11. A. Ma and T. T. Sun, *J. Cell Biol.* **103**, 41 (1986); D. Hohl *et al.*, *J. Biol. Chem.* **266**, 6626 (1991).
12. Probe DH42 corresponds to nt −28 to +248; probe DH36 from +742 to +1693; and probe 3′NC from +2426 to +2604 of the human *TGK* cDNA [H. C. Kim *et al.*, *J. Biol. Chem.* **266**, 536 (1991)].
13. DNA was extracted from blood samples and cell cultures [J. Sambrook, E. G. Fritsch, T. Maniatis,

Molecular Cloning: A Laboratory Manual (Cold Spring Harbor Laboratory, Cold Spring Harbor, NY, ed. 2, 1989)]. The following primers were used for PCR and sequencing (*6*). Exon 2: forward, nt 771 to 791; reverse, nt 1154 to 1173; exon 3: forward, nt 1260 to 1277; reverse, nt 1517 to 1534; exon 6: forward, nt 3323 to 3341; reverse, nt 3544 to 3561; exon 8: forward, nt 4439 to 4456; reverse, nt 4671 to 4690. Forward primers were biotinylated. PCR amplifications were carried out with 2.5 U Taq of DNA polymerase (Gibco BRL) with 30 cycles at 95°C, 45 s; 55°C, 45 s; 72°C, 45 s. PCR products were purified (Magic PCR Preps, Promega), and single-stranded DNA was isolated with streptavidin-coated magnetic beads (Dynal) and sequenced with the reverse primers (Sequenase, U.S. Biochemicals). For SSCP analysis, 1 μCi of ^{32}P-labeled dCTP (deoxycytidine triphosphate) was added to the PCR reaction, and the PCR products were subjected to electrophoresis through a Mutation Detection Enhancement (MDE, AT Biochem) gel in the presence of 10% glycerol at room temperature.

14. RT-PCR was carried out through use of a GeneAmp RNA PCR kit (Perkin-Elmer) (40 cycles at 95°C, 1 min; 55°C, 1 min; 72°C, 1 min). On the basis of human *TGK* cDNA sequence (*12*), the following primers were used: MH4 (nt −49 to −28) and DH4 (nt +818 to +844); DH3 (nt +742 to +758) and DH6 (nt +1667 to +1693); and DH5 (nt +1622 to +1649) and DH7 (nt +2579 to +2604). The reaction products were subcloned into the pGEM-7Z vector and sequenced (Sequenase, U.S. Biochemicals).
15. D. N. Cooper, *Ann. Med.* **25**, 11 (1993).
16. C. Cladaras *et al.*, *J. Biol. Chem.* **262**, 2310 (1986).
17. R. Chakravarty, X. Rong, R. H. Rice, *Biochem. J.* **265**, 25 (1990).
18. R. Chakravarty and R. H. Rice, *J. Biol. Chem.* **264**, 625 (1989).
19. M. A. Phillips, Q. Qin, M. Mehrpouyan, R. H. Rice, *Biochemistry* **32**, 11057 (1993).
20. N. Weraarchakul-Boonmark, J.-M. Jeong, S. N. P. Murthy, J. D. Engel, L. Lorand, *Proc. Natl. Acad. Sci. U.S.A.* **89**, 9804 (1992); F. Tokunaga *et al.*, *J. Biol. Chem.* **268**, 262 (1993).
21. PCR fragments were amplified from genomic DNA of all family members and either digested with restriction enzymes or hybridized to allele-specific oligonucleotides (ASOs). Restriction site polymorphisms were used to characterize the mutations at +1399 (Cfo I site destroyed) and +3459 (Msp I site destroyed) in LI-3, and at +3366 (Msp I site created) in LI-2. ASOs were used to characterize the mutations at +950 (normal: 5′-GCCGTTCCTTCTGG-3′; mutant: 5′-GCCGTTACTTCTGG-3′) in LI-3, and at +4640 (normal: 5′-TTCTGTCTGGTGAGC-3′; mutant: 5′-TTCTGTCGGTGAGC-3′) in LI-1. Nucleotide changes are underlined.
22. H. Mikkola *et al.*, *Blood* **84**, 517 (1994).
23. We thank S. Thacher, B. Rice, and P. Steinert for antibodies and DNA probes; H. Acha-Orbea and D. R. Roop for discussions; J. Rothnagel for PCR sequencing protocols and discussion; C. Scaletta for keratinocyte cultures; L. Bruckner-Tuderman and M. Wyss for patient referrals and samples; and the LI families for their generous support. Supported by funds from the Swiss National Science Foundation grant NF31-36337.92 (to D.H.) and a travel grant from the Spirig Foundation (to M.H.).

2 November 1994; accepted 21 December 1994

Sex Differences in Regional Cerebral Glucose Metabolism During a Resting State

Ruben C. Gur,* Lyn Harper Mozley, P. David Mozley, Susan M. Resnick,† Joel S. Karp, Abass Alavi, Steven E. Arnold, Raquel E. Gur

Positron emission tomography was used to evaluate the regional distribution of cerebral glucose metabolism in 61 healthy adults at rest. Although the profile of metabolic activity was similar for men and women, some sex differences and hemispheric asymmetries were detectable. Men had relatively higher metabolism than women in temporal-limbic regions and cerebellum and relatively lower metabolism in cingulate regions. In both sexes, metabolism was relatively higher in left association cortices and the cingulate region and in right ventro-temporal limbic regions and their projections. These results are consistent with the hypothesis that differences in cognitive and emotional processing have biological substrates.

Sex differences in behavior have been documented across species. In humans, certain sex differences in cognitive and emotional processing are increasingly recognized to have biological substrates. Women perform better than men on some verbal tasks, whereas men excel in certain spatial and motor tasks (*1*). Such differences have been linked to sex hormones (*2*). In the domain of emotional regulation, men are more likely to express affect instrumentally, such as through physical aggression, whereas women use symbolic mediation, such as through vocal means (*3*). Women also have a higher incidence of depression (*4*) and outperform men in emotional discrimination tasks (*5*). In the human brain, sex differences have been found in the size and morphology of the corpus callosum (*6*), preoptic anterior hypothalamic areas (*7*), the bed nucleus of the stria terminalis volume (*8*), sylvian fissure morphology (*9*), the percentage of cortical gray matter tissue, and cerebral blood flow (CBF) rate (*10*).

Theories on brain regulation of human behavior are based primarily on animal experiments, clinical-pathologic correlations, and neurobehavioral studies in healthy persons (*11*). Studies indicate that emotional processing is primarily regulated by the limbic system and closely related areas (*12*), and cognitive functions have been linked to neocortical association areas (*13*). Furthermore, the cerebral hemispheres differ in cognitive and perhaps in emotional processing, with the left specialized for verbal analytic cognition and the right for spatial processing (*14*). There is also evidence for right hemisphere predominance in emotional processing (*15*).

Neuroimaging permits in vivo studies of brain anatomy and physiology pertinent to these issues. Neuroanatomic studies have suggested larger volumes of tissue in left cortical regions implicated in language (*16*), whereas few systematic asymmetries have been reported in neurophysiologic imaging studies (*17*). We examined the regional topography of physiologic activity in healthy young adults using positron emission tomography (PET). Our purpose was to evaluate sex differences in the distribution of cerebral metabolism in limbic regions and to investigate systematic asymmetries that may help us to understand aspects of functional hemispheric specialization.

We studied 61 healthy right-handed volunteers (37 men and 24 women) recruited by advertising. The mean age ± SD was 27.3 ± 6.5 years for men and 27.7 ± 7.4 for women, and the mean years of education ± SD were 14.4 ± 2.0 and 14.9 ± 2.1, respectively. Participants underwent comprehensive medical, neurologic, and psychiatric screenings (*18*). Informed consent was obtained after the nature and possible consequences of the study were explained.

Subjects were scanned after an overnight fast. A radial artery line and a contralateral antebrachium venous line were kept patent with physiological saline. Approximately 185 megabequerels (5 mCi) of ^{18}F-labeled 2-fluoro-2-deoxy-D-glucose (FDG) were administered intravenously while subjects lay in a quiet, dimly lit room with eyes open and ears unoccluded. Subjects were instructed to stay quiet and relaxed without either exerting mental effort or falling asleep (*19*). For determination of the input function, arterial samples were obtained over 90 min. Activity of ^{18}F in 250-μl aliquots was measured in a dose calibrator after a 3- to 4-hour decay interval. Image acquisition began 40 min after isotope administration with the subjects positioned in a custom-molded, head holder of rigid foam that was aligned by two laser beams situated at right angles. The PENN-PET scanner (*20*) has a fixed gantry,

The authors are at the Brain Behavior Laboratory, Neuropsychiatry Section, Department of Psychiatry, and the Center for Functional and Metabolic Imaging, Department of Radiology, University of Pennsylvania School of Medicine, Philadelphia, PA 19104, USA.

*To whom correspondence should be addressed.
†Present address: Gerontology Research Center, National Institute of Aging, Baltimore, MD 21224, USA.